ACS APPLIED MATERIALS & INTERFACES

www.acsami.org

Research Article

General Two-Step Method for the Fabrication of Covalent-Organic Framework-Bound Open-Tubular Capillary Columns for High-Resolution Gas Chromatography Separation of Isomers

Wen-Chao Deng, Hai-Long Qian, Cheng Yang, Shu-Ting Xu, and Xiu-Ping Yan*

Cite This: *ACS Appl. Mater. Interfaces* 2023, 15, 54977−54985

Read Online

ACCESS | Metrics & More | Article Recommendations | Supporting Information

ABSTRACT: Covalent organic frameworks (COFs) are promising as stationary phases for gas chromatography (GC). The successful anchoring of COFs to the inner walls of the capillary with good uniformity is an important prerequisite to ensure the excellent separation performance of columns. However, current methods for the fabrication of COF-based capillary columns cannot always meet this requirement when faced with different COFs, which hampers the further development of COF-based GC stationary phases. Here, we show a general two-step method for the fabrication of COF-bound capillary column. The first step enables the formation of uniform amorphous polymer layer on the inner walls of capillary, while the second step allows the facile transformation of the amorphous polymer layer into a highly crystalline COF layer. COF-bound capillary columns with different framework structures were fabricated successfully by the developed two-step method. Impressively, the COF layers bound on the inner walls of these capillary columns showed good uniformity and high crystallinity. More importantly, as an example, the fabricated Tab-DHTA-bound capillary column showed good resolution (R > 1.5) and high column efficiency (700−39,663 plates m^{-1}) for the tested isomers of ethylbenzene, xylene, dichlorobenzene, chlorotoluene, pinene, 1,3-dichloropropene, and propylbenzene with good precision (RSD, run-to-run, n = 5) (retention time, 0.2−0.6%; peak area, 0.5−1.1%; and peak height, 0.5−1.4%). In general, the fabricated Tab-DHTA-bound capillary column exhibited better performance for the separation isomers than commercial columns DB-5 and HP-FFAP. These results indicate that the two-step method is an efficient way to fabricate the COF-bound capillary column with excellent separation performance.

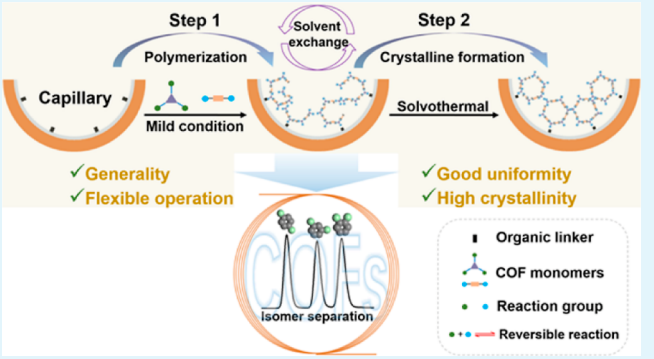

KEYWORDS: *covalent organic frameworks, open-tubular capillary column, two-step method, isomers separation, gas chromatography*

INTRODUCTION

Covalent organic frameworks (COFs) are a new kind of porous materials with ordered pore structures and high crystallinity.[1] The advantages of high chemical stability, adjustable pore size, and easy chemical modification make COFs promising as new stationary phases for a variety of chromatographic separation techniques, such as high-performance liquid chromatography (HPLC), gas chromatography (GC), and capillary electrochromatography (CEC).[2−4] GC with the characteristics of fast analysis and simple operation has been widely used in diverse fields. Since the first COF-coated capillary column was reported for GC separation of alkanes, cyclohexane, benzene, pinene, and alcohols, various framework structures of COFs have been explored to fabricate GC columns with good separation performance.[5−13] Further exploration of the COF-based GC stationary phases with high separation performance is still challenging.

The successful fabrication of a COF open-tubular capillary column is an important prerequisite for further application of COFs in GC separation. Until now, three methods, including "in situ growth",[6,7,13−15] "dynamic coating"[5,8−12], and "silane reagent assisted-chemical bonding",[16] have been developed to fabricate COF open-tubular capillary columns. However, the inherent characteristics of these methods make them not always effective. For "in situ growth", the mixture of the monomers for the synthesis of COF should be first prepared under the optimal solvent condition (such as aqueous acetic acid as catalysis) and then injected into the capillary column to further form COFs. In some cases, the monomers tend to react rapidly to form polymers when the catalyst is added, which

Received: September 15, 2023
Revised: October 26, 2023
Accepted: November 1, 2023
Published: November 14, 2023

may lead to incompetence of "in situ growth" due to the difficult bonding of the aggregated polymers on the inner walls of capillary or even no way to inject the polymers into the capillary with narrow inner diameters (0.25, 0.32, and 0.53 mm). For the other two methods, COF powders, as the starting material, should be first dispersed in a suitable solvent and then anchored to the inner walls of the capillary either through physical attachment or chemical bonding. Therefore, the preparation of homogeneous suspension solution of COFs is critical for the uniform distribution of COFs on the inner walls of capillary. For most COF powders, it is difficult to find an ideal solvent for the homogeneous dispersion of COFs. Meanwhile, the poor dispersion of COF powders in solution may also lead to the severe aggregation of COF particles on the inner walls of the capillary column. These problems with the above methods certainly hamper further wide application and exploration of COFs as stationary phases for GC. Therefore, it is imperative to develop a general method for the preparation of open-tubular capillary columns to overcome the shortcomings of the current fabrication methods.

Reversible condensation (such as the Schiff base reaction) is the main type of reaction to construct high crystalline COFs and gives the formation of COFs as a dynamic reversible process.[3] Previous studies have revealed two stages in the formation of COFs, polymerization, a fast chemical reaction process, and crystalline formation, a slow crystallization process, which is also known as "amorphous to crystalline transformation".[17,18] We speculate that the two stages that come from the COF formation process may be an effective strategy for the fabrication of COF-bound open-tubular capillary columns.

Here, we show a two-step method for the fabrication of COF-bound open-tubular capillary columns for high-resolution GC separation. As a proof-of-concept, a hydroxyl-functionalized 2D COF (Tab-DHTA) prepared from 1,3,5-tris(4-aminophenyl) benzene (Tab) and 2,5-dihydroxy-1,4-benzenedicarboxaldehyde (DHTA) was chosen as a model COF. The proper pore size (3.5 nm), high crystallinity, and rich hydroxyl make Tab-DHTA a potential GC stationary phase.[19,20] The separation of isomers, which is important in various fields but still challenging due to their similar physical and chemical properties, was further carried out to evaluate the separation performance of the Tab-DHTA column.[21,22] Tab-DHTA-bound capillary column shows baseline separation with a high column efficiency, sharp peak shape, and good repeatability for the studied critical isomers (such as ethylbenzene and xylene isomers). This work provides a general method to fabricate COF-bound capillary columns for high-resolution separation.

EXPERIMENTAL SECTION

Materials and Reagents. All of the chemicals used were at least of analytical grade. DHTA, Tab, 4,4′,4″-(1,3,5-triazine-2,4,6-triyl)-trianiline (Tz), and 5,10,15,20-tetrakis(4-aminophenyl)-21*H*,23*H*-porphyrin (Tph) were purchased from Jilin Chinese Academy of Sciences-Yansheng Technology Co. (Changchun, China). Ethylbenzene, *o*-xylene, *p*-xylene, *m*-xylene, *o*-dichlorobenzene (*o*-DCB), *p*-dichlorobenzene, *m*-dichlorobenzene, *o*-chlorotoluene, *p*-chlorotoluene, *m*-chlorotoluene, 1,3,5-trimethylbenzene (mesitylene), *n*-propylbenzene, *iso*-propylbenzene, *n*-alkanes (C5−C12), *n*-alcohols, *n*-esters, benzene, 2-pentanone, 1-nitropropane, pyridine, *n*-butanol (*n*-BuOH), and 3-aminopropyltriethoxysilane (APTES) were purchased from Aladdin Chemistry Co., Ltd. (Shanghai, China). *α*-Pinene, *β*-pinene, *cis*-1,3-dichloropropene, and *trans*-1,3-dichloropropene were purchased from Macklin Bio-Chemical Co. (Shanghai, China). Tetrahydrofuran (THF), 1,4-dioxane, NaOH, *N*,*N*-dimethylformamide (DMF), ethanol (EtOH), methanol (MeOH), hydrochloric acid, and glacial acetic acid (HOAc) were purchased from Sinopharm Chemical Reagent Co., Ltd. (Shanghai, China). Ultrapure water came from Wahaha Foods Co. (Hangzhou, China). Fused silica capillary (0.32 and 0.53 mm i.d.) was purchased from Yongnian Optic Fiber Plant (Hebei, China).

Instrumentation. Powder X-ray diffraction (PXRD) patterns were obtained on a D2 PHASER diffractometer (Bruker AXS GmbH, Germany) with Cu Kα radiation in the range 2−40° (scanning speed 0.1° s^{-1}). Scanning electron microscopy (SEM) images were obtained on an SU8100 scanning electron microscope (Rigaku, Japan). Fourier transform infrared (FT-IR) spectra were obtained on a Nicolet IS20 spectrometer (Nicolet, USA). Thermogravimetric analysis (TGA) was performed on a PTC-10A thermogravimetric analyzer (Rigaku, Japan). N_2 adsorption experiments were performed on an Autosorb-iQ (77 K) (Quantachrome, USA). GC separation was performed on a Shimadzu 2010 Plus system with a flame ionization detector (FID) with nitrogen (99.999%) as the carrier gas.

Two-Step Synthesis of Tab-DHTA, Tz-DHTA, and Tph-DHTA. In step 1, Tab (14.05 mg, 0.04 mmol) and DHTA (9.95 mg, 0.06 mmol) were added to a round-bottom flask and dissolved in 6 mL of *n*-BuOH/THF (1:1, v/v) under ultrasonic conditions. The prepared solution allowed to stand at 90 °C for 4 h. The obtained product was collected by centrifugation, washed with EtOH three times, and then dried at 60 °C under vacuum for 12 h. In step 2, the obtained yellowish powders were transferred into a Pyrex tube (30 mL), and then the mixture of *o*-DCB/*n*-BuOH/6 mol L^{-1} acetic acid aqueous solution (0.5/0.5/0.1 mL) reported in the literature[23] was added into the Pyrex tube. After ultrasonication for 10 min, the suspension was degassed by three freeze−pump−thaw cycles. The tube was sealed and heated at 120 °C for 3 days. The orange color-like precipitate was collected by centrifugation and washed with THF. The powders were dried under vacuum at 60 °C overnight.

Tz-DHTA and Tph-DHTA were prepared in a similar way to Tab-DHTA (see Supporting Information).

Two-Step Fabrication of Tab-DHTA-, Tz-DHTA-, and Tph-DHTA-Bound Open-Tubular Capillary Columns. A bare capillary (0.32 mm i.d. × 15 m long) was pretreated referencing to Qian et al.[6] In step 1, Tab (2.3 mg mL^{-1}) and DHTA (1.65 mg mL^{-1}) were dissolved in a *n*-BuOH/THF (1:1, v/v) solution under ultrasonic conditions. The $-NH_2$ functionalized capillary was filled with the prepared reaction solution and incubated in a water bath at 90 °C for 4 h after both ends were sealed with silicon rubbers. The prepared capillary column was rinsed with EtOH to remove residual solvent and dried with N_2 flow at 70 °C overnight. In step 2, the obtained capillary column was filled with the optimal reaction solvent (*o*-DCB/*n*-BuOH/6 mol L^{-1} acetic acid solution, 1:1:0.2, v/v/v) and incubated in a 120 °C oven for 3 days after both ends were sealed with silicon rubbers. The prepared capillary column was rinsed with THF, filled with THF, and stood in an oven at 60 °C for 8 h to remove unreacted monomers. After the THF was blown out, the capillary column was dried with a N_2 flow for 1 h. Finally, the prepared Tab-DHTA-bound capillary column was conditioned with a temperature program: 70 °C for 10 min, ramp from 70 to 180 °C at a rate of 5 °C min^{-1}, and 180 °C for 1 h.

Tz-DHTA- and Tph-DHTA-bound open-tubular capillary columns were fabricated in a similar way for the Tab-DHTA-bound open-tubular capillary column (see the Supporting Information).

RESULTS AND DISCUSSION

Fabrication and Characterization of COF-Bound Open-Tubular Capillary Columns. The introduction of suitable polar group into COFs can improve the separation performance of COF for isomers (such as C8 compounds).[13,24] Hydroxyl is a multifunctional polar group.[25−27] Although hydroxyl-based COF monomers are easy to obtain, hydroxyl-functionalized COF has not been explored as the

https://doi.org/10.1021/acsami.3c13853
ACS Appl. Mater. Interfaces 2023, 15, 54977−54985

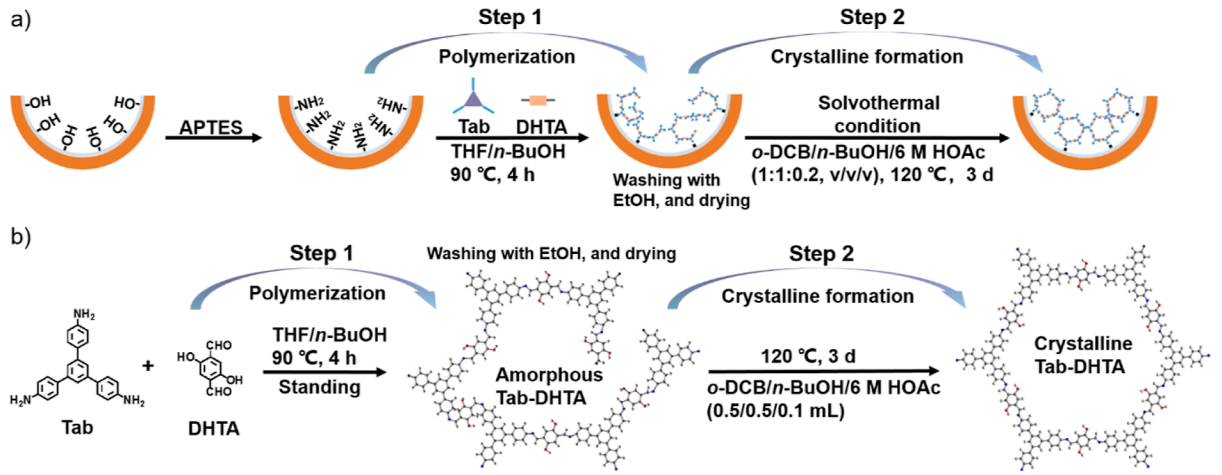

Figure 1. (a) Schematic for the developed two-step method for the fabrication of the Tab-DHTA-bound open-tubular capillary column. (b) Illustration for a two-step synthesis of Tab-DHTA powders.

stationary phase for GC. With this in mind, Tab-DHTA (DHTA can provide two hydroxyls) with a proper pore size (3.5 nm) and high crystallinity was used to demonstrate the two-step fabrication of COF-bound open-tubular capillary columns.[19] In our primary study, conventional methods, such as "in situ growth", "dynamic coating" and "silane reagent assisted-chemical bonding", were applied to fabricate Tab-DHTA-based capillary column, but in vain due to the rapid reaction of Tab and DHTA when the catalyst was added (Figure S1) and the poor dispersion of Tab-DHTA powders in solvents (Figure S2).

In this work, we show a two-step method for the fabrication of a COF-bound capillary column. As illustrated in Figure 1a, a simple polymerization of monomers is designed to prepare an amorphous polymer as the first step. This step plays a main role in the formation of a uniform polymer layer on the inner walls of capillary. As no catalyst is required, the polymerization could avoid the quick reaction, which is a shortcoming for the "in situ growth" method. Meanwhile, as the starting materials, the good solubility or dispersibility of monomers in most common solvents ensures the uniformity of the COF layer on the inner walls of the capillary. These characteristics allow our method to be applied to a variety of COFs.

The crystallinity of COFs is important for the application of COFs as the stationary phase in GC separation.[16,28] So, further transformation of amorphous-to-crystalline is designed as the second step under solvothermal conditions for the fabrication of COF powders to produce a highly crystalline COF layer on the inner walls of capillary column. Before the implementation of the two-step method, the bare capillary is modified with 3-aminopropyltriethoxysilane, which acts as a bridge to connect COFs and capillary through the reaction of Si−O− group on the one side with −OH on the inner surface of capillary and −NH_2 group on the other side with a −CHO group from the monomer. Meanwhile, the uniform distribution of −NH_2 also contributes to the uniform growth of COFs on the inner walls of capillary.

We first investigated a two-step synthesis of Tab-DHTA powders out of a capillary column. We considered the mixture of tetrahydrofuran (THF) with *n*-butanol (*n*-BuOH), *o*-dichlorobenzene (*o*-DCB), or mesitylene as a binary solvent in step 1 for the fabrication of Tab-DHTA powders (Figure 1b). The complete dissolution of Tab and DHTA was achieved in the binary solvents studied containing 50% (v/v) THF. The yields of the products in step 1 were 46.2, 52.5, and 92.9% in THF/mesitylene (1:1, v/v), THF/*o*-DCB (1:1, v/v), and THF/*n*-BuOH (1:1, v/v), respectively. All three binary solvent systems gave amorphous products in step 1 (Figure S3). The obtained amorphous products were further treated under the same solvothermal conditions in step 2 (Figure 1b). Both THF/*o*-DCB and THF/*n*-BuOH binary solvent systems used in step 1 enabled the successful transformation of amorphous-to-crystalline in step 2 out of column (Figure S4). In addition, the reaction temperature and time in step 1 also affected the crystalline formation of the products in step 2 (Figure S5). The best crystallinity of the final product Tab-DHTA in step 2 was obtained when the reaction in step 1 occurred at 90 °C for 4 h.

The as-prepared Tab-DHTA out of column gave a sphere morphology (Figure 2c) with obvious characteristic PXRD peaks of AA stacking at 2.78, 4.73, 5.51, and 7.27° (Figure 2a), which is in good agreement with those reported by Kandambeth et al.[19] FT-IR spectra shows that a new characteristic peak of 1613 cm^{-1} appears to correspond to the imine bond (C═N) stretching (Figure 2b). The Brunauer−Emmet−Teller (BET) surface areas (1137 m^2 g^{-1}) and pore size (3.3 nm) of the prepared Tab-DHTA are similar to the corresponding results reported in the literature,[19] indicating that the two-step method did not change the basic characteristics of Tab-DHTA (Figure 2d,e). In addition, the prepared Tab-DHTA shows good chemical stability in comment solvents for 2 days (Figure S6). Meanwhile, thermal stability up to 400 °C indicates the suitability of Tab-DHTA as the GC stationary phase (Figure 2f).

Based on the above results, we further demonstrated the feasibility of the two-step method for the fabrication of a Tab-DHTA-bound capillary column. As the optimized conditions for the synthesis of Tab-DHTA out of column (Figure S5), a binary solvent THF/*n*-BuOH (1:1, v/v) along with a reaction temperature of 90 °C and a reaction time of 4 h in step 1 gave a uniform amorphous layer on the inner walls of capillary column (Figures S7 and S8), which is in sharp contrast to the bare capillary column (Figure S9). The obtained capillary column was further treated under solvothermal conditions in step 2, as shown in Figure 1a, to transform the Tab-DHTA layer from amorphous into crystalline. The SEM images show

https://doi.org/10.1021/acsami.3c13853
ACS Appl. Mater. Interfaces 2023, 15, 54977−54985

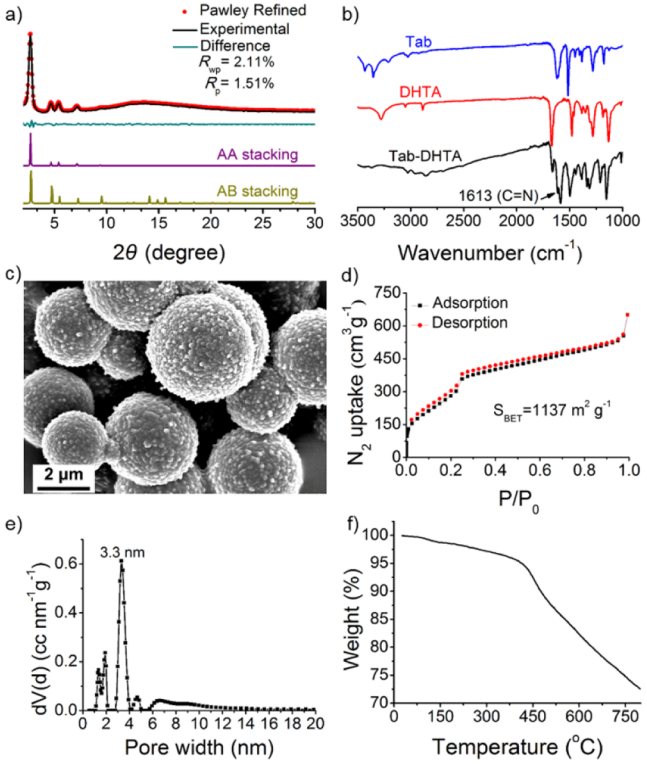

Figure 2. Characterization of Tab-DHTA powders synthesized through the two-step method. (a) Experimental (black) and simulated (purple and dark yellow) PXRD patterns. (b) FT-IR spectra. (c) SEM image. (d) N_2 adsorption−desorption isotherms. (e) Pore size distribution. (f) TGA curve.

that the Tab-DHTA layer bound on the inner walls of the capillary after step 2 was still uniform (Figures 3a,b and S10).

To prove the good crystallinity of the Tab-DHTA grown on the inner walls of the capillary, a Tab-DHTA-bound capillary column with an inner diameter of 0.53 mm (8 m long) was prepared in the same way as shown in Figure 1a. The Tab-DHTA layers scraped from the inner walls of the capillary column gave several characteristic diffraction peaks (2θ: 2.78, 4.73, 5.51, and 7.27°) as the prepared Tab-DHTA out of column (Figure 3c). In addition, the scraped Tab-DHTA layers also gave the FT-IR characteristic peak of Tab-DHTA at 1613 cm^{-1} (C═N) (Figure 3d). These results show the feasibility of the proposed two-step method for the successful fabrication of crystalline Tab-DHTA on the inner walls of the capillary column.

To illustrate the universality of the two-step method, another two kinds of hydroxyl-functionalized COFs (Tz-DHTA[29] and Tph-DHTA[25]) with different symmetries (C3 + C2 and C4 + C2) and pore sizes were used to fabricate capillary columns by our two-step method. PXRD and FT-IR spectrometry proved that both Tz-DHTA and Tph-DHTA were successfully synthesized by the proposed two-step method (Figures S11a,b and S12a,b). Meanwhile, FT-IR spectra (Figures S13 and S14) and SEM images (Figures 3e−h and S15) for the fabricated columns show that Tz-DHTA and Tph-DHTA were bound uniformly on the inner walls of capillary. The results indicate that our two-step method is also promising for the fabrication of other COF-bound capillary columns.

McReynolds Constants of COF-Bound Capillary Columns. Polarity, an important parameter for the separation

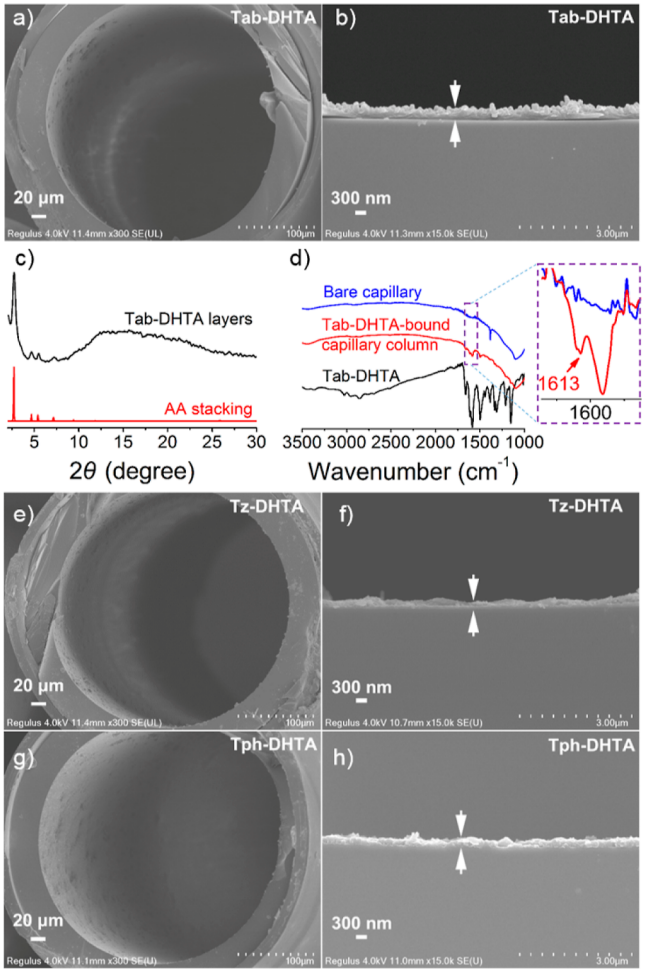

Figure 3. (a,b) Cross-sectional SEM images of Tab-DHTA. (c) PXRD pattern of the Tab-DHTA layers scraped from the inner walls of the capillary column (black) and the simulated PXRD pattern of Tab-DHTA (red). (d) FT-IR spectra of bare capillary, Tab-DHTA-bound capillary column, and Tab-DHTA powders. Cross-sectional SEM images of Tz-DHTA (e,f) and Tph-DHTA (g,h) bound capillary columns.

of analytes on the GC capillary column, is commonly characterized by the McReynolds constants.[30] The five compounds (benzene, *n*-butanol, 1-nitropropane, 2-pentanone, and pyridine) as probe solutes were tested with a column temperature of 120 °C.[31] Table 1 shows the McReynolds constants obtained for the studied COF-bound capillary columns. Both Tab-DHTA and Tph-DHTA-bound capillary columns gave weak polarity, while the other two COF-bound

Table 1. McReynolds Constants of Tab-DHTA-, Tz-DHTA-, Tph-DHTA-, and Amorphous Tab-DHTA-Bound Capillary Columns[a]

columns	X	Y	Z	U	S	average
Tab-DHTA	−49	63	105	67	−67	23.8
Tz-DHTA	−32	179	157	128	80	102.4
Tph-DHTA	−55	81	109	75	−14	39.2
amorphous Tab-DHTA	−27	584	129	105	−12	155.8

[a]Squalane column (0.32 mm i.d. × 15 m long) was fabricated via a dynamic-coating method; X, Y, Z, U, and S represent benzene, *n*-butanol, 2-pentanone, 1-nitropropane, and pyridine, respectively.

https://doi.org/10.1021/acsami.3c13853
ACS Appl. Mater. Interfaces 2023, 15, 54977−54985

capillary columns (Tz-DHTA and amorphous Tab-DHTA) showed moderate polarity. Although the Tab-DHTA and amorphous Tab-DHTA were prepared with the same monomers, amorphous Tab-DHTA provides more residues of $-NH_2$ and $-CHO$ groups for stronger hydrogen bonding interactions with proton−donor analytes, leading to larger polarities than Tab-DHTA.

Separation Performance of Tab-DHTA-Bound Capillary Column. GC separation of different types of important isomers was first conducted to learn the separation performance of Tab-DHTA-bound capillary column. The large pore size of Tab-DHTA allows all the test substances to be accessible to the pore easily without a molecular sieving effect,[32] which makes the separation mainly occur inside the pore. Under the isothermal conditions, all of the tested isomers were baseline separated with a high column efficiency (Figure 4 and Table S1).

As important chemical raw materials, C8 aromatic compounds [ethylbenzene (EB), *m*-xylene (*m*x), *p*-xylene (*p*x), and *o*-xylene (*o*x)] with similar boiling points and molecular dimensions are hard to separate. Even so, our Tab-DHTA-bound capillary column performed with a good resolution ($R_{EB/mx}$ = 3.8, $R_{mx/px}$ = 1.5, and $R_{px/ox}$ = 4.4) and high column efficiency (33,865−39,663 plates m^{-1}). The elution sequence is not exactly consistent with the boiling points of these compounds. *o*-Xylene has the longest retention time, which may be ascribed to its highest boiling point and the interaction between its two methyl groups and the hydroxyl groups from the frameworks at the same time.[20,22] EB with the lowest boiling point is the earliest to be eluted. For p- and m-xylene, the pore-filling effect lokely dominates their separation.[33]

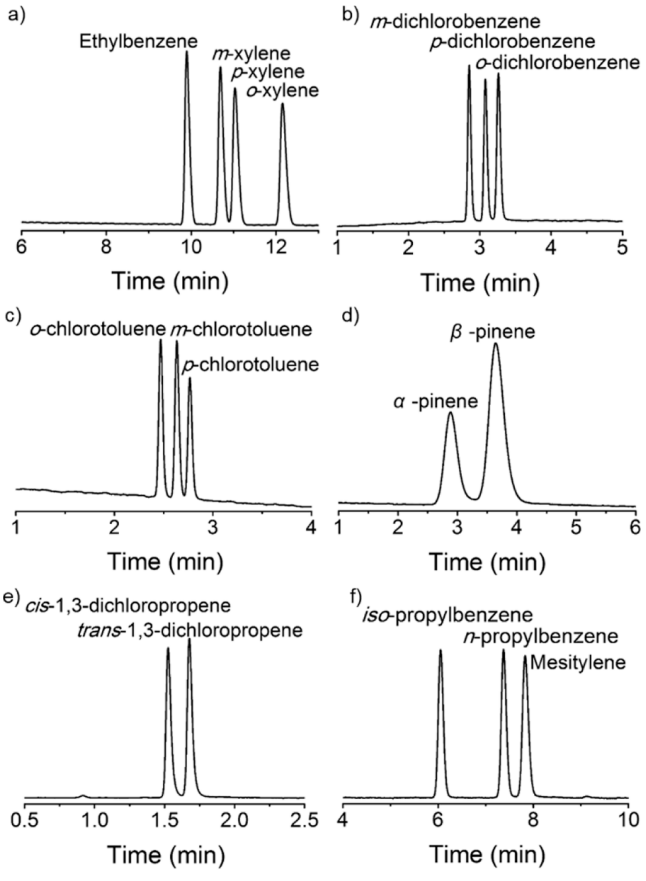

Figure 4. GC chromatograms on the Tab-DHTA-bound capillary column (0.32 mm inner diameter × 15 m long). Analytes and separation conditions: (a) ethylbenzene and xylene isomers, 170 °C, 1.4 mL min^{-1} (N_2 flow); (b) dichlorobenzene isomers, 210 °C, 2.0 mL min^{-1} (N_2 flow); (c) chlorotoluene isomers, 220 °C, 1.6 mL min^{-1} (N_2 flow); (d) pinene isomers, 210 °C, 1.8 mL min^{-1} (N_2 flow); (e) 1,3-dichloropropene isomers, 200 °C, 1.2 mL min^{-1} (N_2 flow); and (f) propylbenzene isomers, 190 °C, 1.8 mL min^{-1} (N_2 flow).

The other studied isomers [dichlorobenzene (*o*-, *p*-, *m*-), chlorotoluene (*o*-, *p*-, *m*-), pinene (*α*-, *β*-), propylbenzene (1,3,5-trimethylbenzene, *n*-propylbenzene, *iso*-propylbenzene), and 1,3-dichloropropene (*cis*-, *trans*-)] were also baseline separated with a short retention time and high column efficiency (700−18,645 plates m^{-1}) (Figure 4b−f and Table S1). The elution sequences of different configurations of isomers are all in good accordance with the increasing order of the boiling points. The baseline separation of the tested isomers based on the boiling point indicates that the van der Waals force plays a main role in separation.[33] Meanwhile, the other interactions between analytes and Tab-DHTA, such as $\pi-\pi$ interactions[5,34] and hydrogen bonding interactions,[7,21] may also contribute to separation. Besides isomers, *n*-alkanes, *n*-alcohols, and *n*-esters with a wide range of boiling points were also baseline separated on the Tab-DHTA-bound capillary column in an increasing order of boiling point (Figure S16). For *n*-alkanes, van der Waals force contributed to their baseline separation.[7,21,34] Besides van der Waals force, the hydrogen bonding interaction may also contribute to the baseline separation of *n*-alcohols and *n*-esters.[5,7]

The repeatability and stability of the Tab-DHTA-bound capillary column were evaluated with C8 compounds and dichlorobenzene (*o*-, *p*-, *m*-) as the analytes. The relative standard deviations (RSDs) of retention time, peak area, peak high, and half peak width for run-to-run (n = 5) (0.2−0.6, 0.5−1.1, 0.5−1.4, and 1.2−2.4% respectively) and day-to-day (n = 5) (1.4−2.2, 0.8−2.7, 1.7−3.9, and 1.8−2.4% respectively) reveal the good repeatability of Tab-DHTA-bound capillary column (Table S2). In addition, the column-to-column RSDs (n = 3) for retention time, peak area, peak high, and half peak width were 6.0−6.5, 2.0−3.2, 3.5−6.3, and 4.9−8.6%, respectively (Table S2), indicating the reliability of the two-step method. A slight fluctuation of column efficiency was observed after the column was treated through a temperature-programmed process (Figure S17), and the COF layer remained intact (Figure S18), indicating the good stability of the COF layer. All the above results strongly show the excellent performance of our two-step method for the fabrication of COF-bound capillary column.

The thermodynamics for the separation on the Tab-DHTA-bound capillary column was further studied. Ethylbenzene, xylene (*o*-, *p*-, *m*-), dichlorobenzene (*o*-, *p*-, *m*-), chlorotoluene (*o*-, *p*-, *m*-), and 1,3-dichloropropene (*cis*-, *trans*-) were chosen as the analytes. The good linearity of van't Hoff plots for the tested isomers (Figure S19) shows the unchanged interaction mechanism in the temperature range studied. The values of enthalpy change (ΔH), entropy change (ΔS), and Gibbs free energy change (ΔG) calculated from the van't Hoff equation are summarized in Table S3. The separation of all of the tested isomers on the Tab-DHTA-bound capillary column was controlled by both ΔH and ΔS. Meanwhile, the negative

https://doi.org/10.1021/acsami.3c13853
ACS Appl. Mater. Interfaces 2023, 15, 54977−54985

value of ΔG indicates that the separation is a thermodynamic spontaneous process.

Importance of the Two-Step Method. To show the necessity of the two steps in our method, we fabricated an amorphous Tab-DHTA-bound capillary column in the absence of step 2 (see Supporting Information). Then, the amorphous Tab-DHTA-bound capillary column was compared with the above crystalline Tab-DHTA-bound capillary column for the separation of isomers. Unfortunately, no baseline separation was observed for all the studied isomers on the amorphous Tab-DHTA-bound capillary column under the same separation conditions for the crystalline Tab-DHTA-bound capillary column (Figure S20). Meanwhile, the amorphous Tab-DHTA-bound capillary column gave the distinct broad and tailing chromatographic peaks. Even under the optimal separation conditions, only 1,3-dichloropropene isomers were baseline separated (Figure S21). In addition, baseline separation of *n*-alkanes, *n*-alcohols, and *n*-esters was achieved on the amorphous Tab-DHTA-bound capillary column under the optimized condition of programmed temperature (Figure S21g–i). Obviously, these results indicate a key role of step 2 in the improvement of the separation performance of the Tab-DHTA-bound capillary column. In addition, except for pinene isomers, other studied isomers were not baseline separated on the bare capillary column modified with APTES (Figure S22), indicating the important role of COF in isomer separation.

To understand the difference in separation performance between the amorphous and crystalline Tab-DHTA-bound capillary columns, we studied the thermodynamics and kinetics for the separation on both columns. Dichlorobenzene isomers were chosen as analytes for this purpose. From a thermodynamic point of view, the amorphous Tab-DHTA-bound capillary column gave more negative values of ΔH and ΔS than crystalline Tab-DHTA-bound capillary column for each individual isomer (Tables S3 and S4), suggesting stronger interactions of the isomers with the amorphous Tab-DHTA-bound capillary column due likely to the larger Y value (a strong hydrogen bonding ability) of the amorphous Tab-DHTA-bound capillary column (Table 1). However, no significant difference in ΔH and ΔS for *o*-, *m*-, and *p*-dichlorobenzene either on amorphous (Table S4) or crystalline (Table S3) Tab-DHTA-bound capillary columns indicates a similar selectivity difference for the three configurations on both columns. Thus, thermodynamics did not dominate the difference in separation performance between amorphous and crystalline Tab-DHTA-bound capillary columns.

The separation kinetics was then studied using the Golay equation ($H = B/u + C \times u$, where H is the height equivalent to a theoretical plate (HETP), B is the coefficient of longitudinal diffusion, C is the coefficient of mass-transfer resistance, and u is the linear velocity of the mobile phase). As shown in Figure S23, no complete Golay plot was obtained on the amorphous Tab-DHTA-bound capillary column, as the optimal velocity (u_{opt}) of the mobile phase was lower than the minimum allowable velocity of the mobile phase in GC. So, it is not possible to compare B and C on both columns. Nevertheless, the greater HETP on the amorphous Tab-DHTA-bound capillary column revealed the lower column efficiency than the crystalline Tab-DHTA-bound capillary column (Figure S23). HETP is related to the diffusion and mass transport of analytes. The similar uniformity and thickness (300 nm) of the COF layer on both columns illustrated that the diffusion of analytes on both columns was similar (Figures 3a,b vs S8).[35] So, the greater HETP on the amorphous Tab-DHTA-bound capillary column should be aroused by the mass transport resistance. Amorphous Tab-DHTA had a lower BET surface area (84.5 $m^2\ g^{-1}$) (Figure S24) and lower pore volume (0.095 $cm^3\ g^{-1}$) at $P/P_0 = 0.99$ but still had 2 nm pores (Figure S24b), which means that the separation on the amorphous Tab-DHTA-bound capillary column could occur on the inside of the pore. However, compared with crystalline Tab-DHTA, amorphous Tab-DHTA had a disordered pore structure, which could be an obstacle for the transport of analyte inside the pore and further lead to the large mass-transfer resistance. The above results indicate that the mass transport of the analytes dominated the difference in the separation performance between amorphous and crystalline Tab-DHTA-bound capillary columns. In general, the crystalline Tab-DHTA with ordered pores is more favorable for the separation of the tested isomers, which was also shown on COF-based stationary phases for the separation of chiral compounds.[16,27]

Separation Performance of Tz-DHTA- and Tph-DHTA-Bound Capillary Columns. The good thermal and chemical stabilities of Tz-DHTA (Figures S8e and S25a) and Tph-DHTA (Figures S9e and S25b) also encouraged us to study the separation performance of Tz-DHTA- and Tph-DHTA-bound capillary columns. EB, xylene, chlorotoluene, and pinene isomers were chosen as the analytes. Under the isothermal conditions, both columns had the ability to separate the isomers with a high column efficiency (2146–25,876 plates m^{-1}) (Figure 5 and Table S1). The elution sequences of the isomers are in accordance with the increasing order of the boiling points. These results further illustrate the reliability and the generality of the developed two-step method. Similar to Tab-DHTA, the large pore sizes of Tz-DHTA (2.59 nm) (Figure S11d) and Tph-DHTA (1.78 nm) (Figure S12d) made the separation mainly occur inside the pore. In addition, the use of DHTA with a hydroxyl group made Tab-DHTA, Tz-DHTA, and Tph-DHTA have a similar pore chemical environment. However, the separation performance of these columns is significantly different. For example, the baseline separation of EB, xylene, and chlorotoluene isomers was not achieved on the Tz-DHTA-bound capillary column. Among the three capillary columns studied, the Tph-DHTA-bound capillary column gave the best separation performance for the tested isomers. In particular, EB and xylene isomers were baseline separated within 4.6 min with a high column efficiency (21,351–25,876 plates m^{-1}) and good resolution ($R_{EB/mx}$ = 2.2, $R_{mx/px}$ = 1.6, and $R_{px/ox}$ = 3.1), which outperforms the reported 2D COF and other porous material-based GC stationary phases (Table S5).[7,21,24,33,34,36,37]

Comparison with Commercial Capillary Columns. Further comparison of the Tab-DHTA-bound capillary column (0.53 mm inner diameter × 10 m long) with two commercial columns DB-5 and HP-FFAP (0.53 mm inner diameter × 10 m long) was made. Our Tab-DHTA-bound capillary column enabled the baseline separation of more isomers tested (Figures S26–S28) with a comparable column efficiency to the two commercial columns except for pinene isomers (Table S6). For example, the Tab-DHTA-bound capillary column gave the baseline separation of chlorotoluene isomers ($R_{o/m}$ = 2.0 and $R_{m/p}$ = 1.5), but DB-5 ($R_{o/m}$ = 0.0 and $R_{m/p}$ = 0.2) and HP-FFAP columns ($R_{o/m}$ = 1.5 and $R_{m/p}$ = 0.0) did not. Meanwhile, the Tab-DHTA-bound capillary column showed

https://doi.org/10.1021/acsami.3c13853
ACS Appl. Mater. Interfaces 2023, 15, 54977–54985

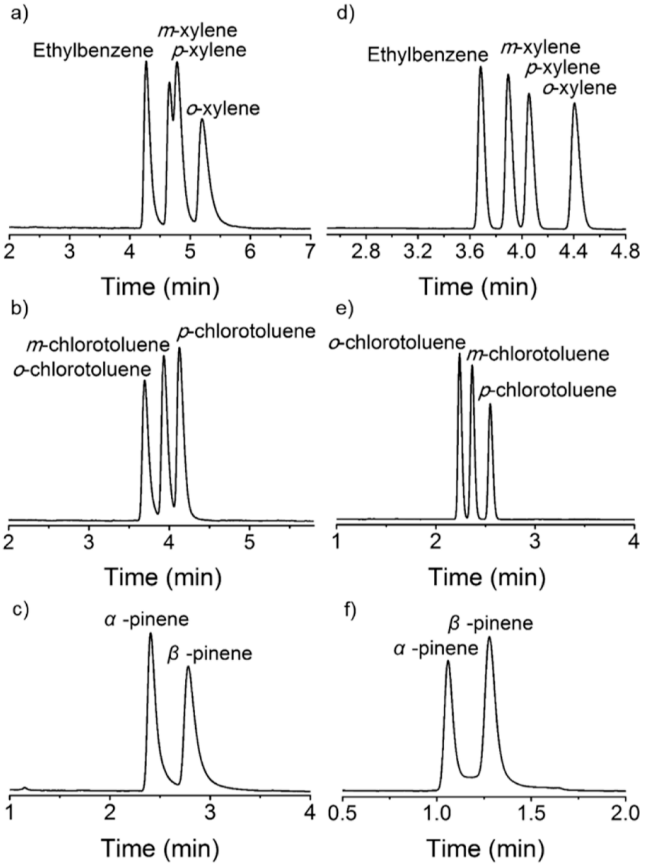

Figure 5. GC chromatograms on Tz-DHTA (a–c)- and Tph-DHTA (d–f)-bound capillary columns (0.32 μm i.d. × 15 m long). Analytes and separation conditions: (a) ethylbenzene and xylene isomers, 150 °C, 1.1 mL min^{-1} (N_2 flow); (b) chlorotoluene isomers, 170 °C, 1.0 mL min^{-1} (N_2 flow); (c) pinene isomers, 190 °C, 1.0 mL min^{-1} (N_2 flow); (d) ethylbenzene and xylene isomers, 185 °C, 1.54 mL min^{-1} (N_2 flow); (e) chlorotoluene isomers, 205 °C, 2.0 mL min^{-1} (N_2 flow); and (f) pinene isomers, 240 °C, 2.5 mL min^{-1} (N_2 flow).

better separation performance for dichlorobenzene isomers ($R_{m/p}$ = 2.0 and $R_{p/o}$ = 1.5) than the DB-5 column ($R_{m/p}$ = 1.2 and $R_{p/o}$ = 2.5). As the increase of column diameter (from 0.32 to 0.53 mm) and decrease of column length (from 15 to 10 m) led to the decrease of the column efficiency, no baseline separation of *m*- and *p*-xylene was achieved on Tab-DHTA column (0.53 mm i.d. × 10 m long). Although EB and xylene isomers were not baseline separated on the above three columns, the Tab-DHTA-bound capillary column gave better resolution between EB, *m*-, and *p*-xylene ($R_{EB/mx}$ = 2.0 and $R_{mx/px}$ = 0.8) than the DB-5 column ($R_{EB/px}$ = 1.6 and $R_{px/mx}$ = 0.0) and HP-FFAP column ($R_{EB/px}$ = 1.3). Detailed resolution data for the separation of the tested isomers on the three columns are summarized in Table S7. The above results not only reveal the potential of hydroxyl-functionalized COF as a stationary phase for GC but also the great potential of developed two-step method in the fabrication of COF-bound capillary columns with high separation performance.

CONCLUSIONS

In summary, we have successfully developed a general two-step method for the fabrication of COF-bound open-tubular capillary columns. This method allows the fabrication of uniform and highly crystalline COF layers bound on the inner walls of the capillary for high-resolution GC separation. More importantly, the fabricated COF-bound capillary columns showed good separation performance and repeatability for the critical isomers studied. Meanwhile, this work shows the great potential of hydroxyl-functionalized COFs as a GC stationary phase (such as porphyrin-based COF Tph-DHTA). The developed two-step method will promote the fabrication of more and more COF-bound open-tubular capillary columns with good separation performance for GC. In addition, our method is also promising for fabricating COF-bound open-tubular capillary columns for capillary electrochromatography, another important chromatography technology.

ASSOCIATED CONTENT

Supporting Information

The Supporting Information is available free of charge at https://pubs.acs.org/doi/10.1021/acsami.3c13853.

Methods; calculation; photos of Tab-DHTA prepolymerization solution before and after the catalyst was added; photos of the dispersion state of Tab-DHTA in different solvents; PXRD patterns; effect of binary solvents used in step 1 on the crystallinity of finial products in step 2; effect of reaction temperatures and times in step 1 on the crystallinity of the products in step 2; chemical stability of Tab-DHTA; SEM images; characterization of Tz-DHTA and Tph-DHTA powders and capillary columns; stability of Tab-DHTA layer; GC chromatograms and Van't Hoff plots on the crystalline Tab-DHTA-bound capillary column; GC chromatograms; Golay plots on amorphous and crystalline Tab-DHTA-bound capillary columns; characterization of amorphous Tab-DHTA powders; chemical stability of Tz-DHTA and Tph-DHTA; column efficiency and resolution of Tab-DHTA-, Tz-DHTA-, and Tph-DHTA-bound capillary columns; precision of Tab-DHTA-bound capillary column; thermodynamic parameters for amorphous and crystalline Tab-DHTA-bound capillary columns; comparison of separation performance of Tph-DHTA column and other stationary phase in references; and comparison of column efficiency and resolution on Tab-DHTA, DB-5, and HP-FFAP columns (PDF)

AUTHOR INFORMATION

Corresponding Author

Xiu-Ping Yan − *State Key Laboratory of Food Science and Resources, Jiangnan University, Wuxi 214122, China; International Joint Laboratory on Food Safety, Institute of Analytical Food Safety, School of Food Science and Technology, and Key Laboratory of Synthetic and Biological Colloids, Ministry of Education, School of Chemical and Material Engineering, Jiangnan University, Wuxi 214122, China;* orcid.org/0000-0001-9953-7681; Email: xpyan@jiangnan.edu.cn

Authors

Wen-Chao Deng − *State Key Laboratory of Food Science and Resources, Jiangnan University, Wuxi 214122, China; International Joint Laboratory on Food Safety and Institute of Analytical Food Safety, School of Food Science and Technology, Jiangnan University, Wuxi 214122, China*

Hai-Long Qian − *State Key Laboratory of Food Science and Resources, Jiangnan University, Wuxi 214122, China;*

International Joint Laboratory on Food Safety and Institute of Analytical Food Safety, School of Food Science and Technology, Jiangnan University, Wuxi 214122, China; orcid.org/0000-0001-7554-4115

Cheng Yang − *Institute of Analytical Food Safety, School of Food Science and Technology, Jiangnan University, Wuxi 214122, China*

Shu-Ting Xu − *State Key Laboratory of Food Science and Resources, Jiangnan University, Wuxi 214122, China; International Joint Laboratory on Food Safety and Institute of Analytical Food Safety, School of Food Science and Technology, Jiangnan University, Wuxi 214122, China*

Complete contact information is available at: https://pubs.acs.org/10.1021/acsami.3c13853

Author Contributions

Wen-Chao Deng: conceptualization, investigation, data curation, validation, and writing—original draft. Hai-Long Qian: validation. Cheng Yang: validation. Shu-Ting Xu: validation. Xiu-Ping Yan: conceptualization, project administration, writing—review and editing, funding acquisition, and supervision.

Notes

The authors declare no competing financial interest.

■ ACKNOWLEDGMENTS

This work was supported by the National Natural Science Foundation of China (nos. 22176073 and 22076066) and the Program of "Collaborative Innovation Center of Food Safety and Quality Control in Jiangsu Province".

■ REFERENCES

(1) Feng, X.; Ding, X. S.; Jiang, D. L. Covalent Organic Frameworks. *Chem. Soc. Rev.* **2012**, *41*, 6010−6022.

(2) Ding, S. Y.; Wang, W. Covalent Organic Frameworks (COFs): from Design to Applications. *Chem. Soc. Rev.* **2013**, *42*, 548−568.

(3) Kandambeth, S.; Dey, K.; Banerjee, R. Covalent Organic Frameworks: Chemistry Beyond the Structure. *J. Am. Chem. Soc.* **2019**, *141*, 1807−1822.

(4) Qian, H. L.; Yang, C. X.; Wang, W. L.; Yang, C.; Yan, X. P. Advances in Covalent Organic Frameworks in Separation Science. *J. Chromatogr. A* **2018**, *1542*, 1−18.

(5) Yang, C. X.; Liu, C.; Cao, Y. M.; Yan, X. P. Facile Room Temperature Solution-Phase Synthesis of a Spherical Covalent Organic Framework for High-Resolution Chromatographic Separation. *Chem. Commun.* **2015**, *51*, 12254−12257.

(6) Qian, H. L.; Yang, C. X.; Yan, X. P. Bottom-Up Synthesis of Chiral Covalent Organic Frameworks and Their Bound Capillaries for Chiral Separation. *Nat. Commun.* **2016**, *7*, 12104.

(7) Huang, X. L.; Lan, H. H.; Yan, Y. L.; Chen, G.; He, Z. H.; Zhang, K.; Cai, S. L.; Zheng, S. R.; Fan, J.; Zhang, W. G. Fabrication of a Hydrazone-Linked Covalent Organic Framework-Bound Capillary Column for Gas Chromatography Separation. *Sep. Sci. plus* **2019**, *2*, 120−128.

(8) Guo, J. X.; Yang, C.; Yan, X. P. Thiol-ene Click Synthesis of Chiral Covalent Organic Frameworks for Gas Chromatography. *J. Mater. Chem. A* **2021**, *9*, 21151−21157.

(9) Tang, B.; Wang, W.; Hou, H. P.; Liu, Y. Q.; Liu, Z. K.; Geng, L. N.; Sun, L. Q.; Luo, A. Q. A *β*-cyclodextrin Covalent Organic Framework Used as a Chiral Stationary Phase for Chiral Separation in Gas Chromatography. *Chin. Chem. Lett.* **2022**, *33*, 898−902.

(10) Yuan, C.; Jia, W. Y.; Yu, Z. Y.; Li, Y. N.; Zi, M.; Yuan, L. M.; Cui, Y. Are Highly Stable Covalent Organic Frameworks the Key to Universal Chiral Stationary Phases for Liquid and Gas Chromatographic Separations? *J. Am. Chem. Soc.* **2022**, *144*, 891−900.

(11) Wang, Z.; Xiong, W. Q.; Huang, Z. F.; Qin, G. Z.; Zi, M.; Yuan, L. M. Chiral Derivatives of Covalent Organic Framework TpBD $(NH_2)_2$ Used as Stationary Phases in Gas Chromatography. *Chirality* **2022**, *34*, 462−472.

(12) Ma, T. T.; Yang, C.; Qian, H. L.; Yan, X. P. Post-Modification of Covalent Organic Framework for Gas Chromatographic Separation of Isomers. *J. Chromatogr. A* **2022**, *1673*, 463085.

(13) Qian, H. L.; Wang, Z. H.; Yang, J.; Yan, X. P. Building-Block Exchange Synthesis of Amino-Based Three-Dimensional Covalent Organic Framework for Gas Chromatographic Separation of Isomers. *Chem. Commun.* **2022**, *58*, 8133−8136.

(14) Kong, D. Y.; Bao, T.; Chen, Z. L. In Situ Synthesis of the Imine-Based Covalent Organic Framework LZU1 on the Inner Walls of Capillaries for Electrochromatographic Separation of Nonsteroidal Drugs and Amino Acids. *Microchim. Acta* **2017**, *184*, 1169−1176.

(15) Li, Y. J.; Lin, X. T.; Qin, S. L.; Gao, L. D.; Tang, Y. M.; Liu, S. R.; Wang, Y. Y. *β*-Cyclodextrin-Modified Covalent Organic Framework as Chiral Stationary Phase for the Separation of Amino Acids and *β*-Blockers by Capillary Electrochromatography. *Chirality* **2020**, *32*, 1008−1019.

(16) Wang, G. X.; Lv, W. J.; Pan, C. J.; Chen, H. L.; Chen, X. G. Synthesis of a Novel Chiral DA-TD Covalent Organic Framework for Open-Tubular Capillary Electrochromatography Enantioseparation. *Chem. Commun.* **2022**, *58*, 403−406.

(17) Gao, Q.; Bai, L. Y.; Zeng, Y. F.; Wang, P.; Zhang, X. J.; Zou, R. Q.; Zhao, Y. L. Reconstruction of Covalent Organic Frameworks by Dynamic Equilibrium. *Chem.—Eur. J.* **2015**, *21*, 16818−16822.

(18) Smith, B. J.; Overholts, A. C.; Hwang, N.; Dichtel, W. R. Insight into the Crystallization of Amorphous Imine-Linked Polymer Networks to 2D Covalent Organic Frameworks. *Chem. Commun.* **2016**, *52*, 3690−3693.

(19) Kandambeth, S.; Venkatesh, V.; Shinde, D. B.; Kumari, S.; Halder, A.; Verma, S.; Banerjee, R. Self-Templated Chemically Stable Hollow Spherical Covalent Organic Framework. *Nat. Commun.* **2015**, *6*, 6786.

(20) Huang, J. J.; Han, X.; Yang, S.; Cao, Y. Y.; Yuan, C.; Liu, Y.; Wang, J. G.; Cui, Y. Microporous 3D Covalent Organic Frameworks for Liquid Chromatographic Separation of Xylene Isomers and Ethylbenzene. *J. Am. Chem. Soc.* **2019**, *141*, 8996−9003.

(21) Fang, Z. L.; Zheng, S. R.; Tan, J. B.; Cai, S. L.; Fan, J.; Yan, X.; Zhang, W. G. Tubular Metal-Organic Framework-Based Capillary Gas Chromatography Column for Separation of Alkanes and Aromatic Positional Isomers. *J. Chromatogr. A* **2013**, *1285*, 132−138.

(22) Yang, C. X.; Liu, S. S.; Wang, H. F.; Wang, S. W.; Yan, X. P. High-Performance Liquid Chromatographic Separation of Position Isomers Using Metal-Organic Framework MIL-53(Al) as the Stationary Phase. *Analyst* **2012**, *137*, 133−139.

(23) Xu, H.; Gao, J.; Jiang, D. Stable, Crystalline, Porous, Covalent Organic Frameworks as a Platform for Chiral Organocatalysts. *Nat. Chem.* **2015**, *7*, 905−912.

(24) Ma, T. T.; Yang, C.; Qian, H. L.; Ma, P. M.; Liu, T. X.; Yan, X. P. Trifluoromethyl-Functionalized 2D Covalent Organic Framework for High-Resolution Separation of Isomers. *ACS Appl. Mater. Interfaces* **2023**, *15*, 32926−32934.

(25) Kandambeth, S.; Shinde, D. B.; Panda, M. K.; Lukose, B.; Heine, T.; Banerjee, R. Enhancement of Chemical Stability and Crystallinity in Porphyrin-Containing Covalent Organic Frameworks by Intramolecular Hydrogen Bonds. *Angew. Chem., Int. Ed.* **2013**, *52*, 13052−13056.

(26) Du, M. L.; Yang, C.; Qian, H. L.; Yan, X. P. Hydroxyl-Functionalized Three-Dimensional Covalent Organic Framework for Selective and Rapid Extraction of Organophosphorus Pesticides. *J. Chromatogr. A* **2022**, *1673*, 463071.

(27) Lu, Q. Y.; Ma, Y. C.; Li, H.; Guan, X. Y.; Yusran, Y.; Xue, M.; Fang, Q. R.; Yan, Y. S.; Qiu, S. L.; Valtchev, V. Postsynthetic Functionalization of Three-Dimensional Covalent Organic Frameworks for Selective Extraction of Lanthanide Ions. *Angew. Chem., Int. Ed.* **2018**, *57*, 6042.

(28) Han, X.; Huang, J. J.; Yuan, C.; Liu, Y.; Cui, Y. Chiral 3D Covalent Organic Frameworks for High Performance Liquid Chromatographic Enantioseparation. *J. Am. Chem. Soc.* **2018**, *140*, 892−895.
(29) Sun, B.; Liu, J.; Cao, A. M.; Song, W. G.; Wang, D. Interfacial Synthesis of Ordered and Stable Covalent Organic Frameworks on Amino-Functionalized Carbon Nanotubes with Enhanced Electrochemical Performance. *Chem. Commun.* **2017**, *53*, 6303−6306.
(30) Berthod, A.; Zhou, E. Y.; Le, K.; Armstrong, D. W. Determination and Use of Rohrschneider-McReynolds Constants for Chiral Stationary Phases Used in Capillary Gas Chromatography. *Anal. Chem.* **1995**, *67*, 849−857.
(31) McReynolds, W. O. Characterization of some Liquid Phases. *J. Chromatogr. Sci.* **1970**, *8*, 685−691.
(32) Chang, N.; Gu, Z. Y.; Yan, X. P. Zeolitic Imidazolate Framework-8 Nanocrystal Coated Capillary for Molecular Sieving of Branched Alkanes from Linear Alkanes along with High-Resolution Chromatographic Separation of Linear Alkanes. *J. Am. Chem. Soc.* **2010**, *132*, 13645−13647.
(33) Lu, C. M.; Liu, S. Q.; Xu, J. Q.; Ding, Y. J.; Ouyang, G. F. Exploitation of a Microporous Organic Polymer as a Stationary Phase for Capillary Gas Chromatography. *Anal. Chim. Acta* **2016**, *902*, 205−211.
(34) Chang, N.; Yan, X. P. Exploring Reverse Shape Selectivity and Molecular Sieving Effect of Metal-Organic Framework UIO-66 Coated Capillary Column for Gas Chromatographic Separation. *J. Chromatogr. A* **2012**, *1257*, 116−124.
(35) Reid, V. R.; Synovec, R. E. High-Speed Gas Chromatography: the Importance of Instrumentation Optimization and the Elimination of Extra-Column Band Broadening. *Talanta* **2008**, *76*, 703−717.
(36) Li, H. X.; Xie, T. P.; Yan, K. Q.; Xie, S. M.; Wang, B. J.; Zhang, J. H.; Yuan, L. M. A Hydroxyl-Functionalized Homochiral Porous Organic Cage for Gas Chromatographic Separations. *Microchim. Acta* **2020**, *187*, 269.
(37) Münch, A. S.; Mertens, F. O. R. L. HKUST-1 as an Open Metal Site Gas Chromatographic Stationary Phase—Capillary Preparation, Separation of Small Hydrocarbons and Electron Donating Compounds, Determination of Thermodynamic Data. *J. Mater. Chem.* **2012**, *22*, 10228−10234.

https://doi.org/10.1021/acsami.3c13853
ACS Appl. Mater. Interfaces 2023, 15, 54977−54985